Symmetry properties of natural frequency and mode shape sensitivities in symmetric structures

Published article available online: Mechanical Systems and Signal Processing 143 (2020) 106797

Daniel T. Bartilson[a,*], Jinwoo Jang[b], Andrew W. Smyth[a]

[a]Department of Civil Engineering and Engineering Mechanics, Columbia University, New York, NY 10027, USA
[b]Department of Civil, Environmental & Geomatics Engineering, Florida Atlantic University, Boca Raton, FL 33431, USA

Abstract

When updating a finite element (FE) model to match the measured properties of its corresponding structure, the sensitivities of FE model outputs to parameter changes are of significant interest. These sensitivities form the core of sensitivity-based model updating algorithms, but they are also used for developing reduced parametrizations, such as in subset selection and clustering. In this work, the sensitivities of natural frequencies and mode shapes are studied for structures having at least one plane of reflectional symmetry. It is first shown that the mode shapes of these structures are either symmetric and anti-symmetric, which is used to prove that natural frequency sensitivities are equal for symmetric parameters. Conversely, mode shape sensitivities are shown to be unequal for symmetric parameters, as measured by cosine distance. These topics are explored with a small numerical example, where it is noted that mode shape sensitivities for symmetric parameters exhibit similar properties to asymmetric parameters.

Keywords: Modal analysis, Sensitivity-based model updating, Eigenvalue problem, Symmetry, Sensitivity analysis

1. Introduction

Finite element (FE) models are of great importance in science and engineering for modeling of physical systems. In structural engineering, an FE model generally corresponds to a unique physical structure but there may exist significant discrepancy between measured and model-predicted behavior. The presence of discrepancy limits the predictive value of an FE model. FE model updating seeks to reduce discrepancy between measured and model-output behavior, often modal properties, by adjusting parameters of an FE model, such as element masses and stiffnesses [1]. An excellent review of model updating, encompassing contemporary methods in uncertainty quantification, is available by Simoen *et al.* [2].

One of the most popular and intuitive methods for FE model updating is the sensitivity method [1] which uses a series of linear approximations to minimize a non-linear sum-of-square error function between measured and model-output data vectors. In the linear approximation step, the sensitivity method directly utilizes the Jacobian matrix, also called the sensitivity matrix, which captures the derivatives of model outputs with respect to parameter changes [1]. The condition of the sensitivity matrix is of paramount importance to the sensitivity method, since parameters are updated using the pseudo-inverse of the sensitivity matrix. Poor conditioning occurs when there are more unknowns (parameters to update) than equations (measurements), but can also result from noisy data or poor selection of updating parameters [1].

Two general approaches have been adopted for improving the condition of the sensitivity matrix in FE model updating: regularization and reduced parametrization. Regularization has been widely studied and utilized in FE model updating [1, 3–5], and involves adding equations to constrain the amount of

*Corresponding author
Email addresses: dtb2121@columbia.edu (Daniel T. Bartilson), jangj@fau.edu (Jinwoo Jang), smyth@civil.columbia.edu (Andrew W. Smyth)
URL: http://faculty.eng.fau.edu/jangj/ (Jinwoo Jang), http://www.columbia.edu/cu/civileng/smyth/ (Andrew W. Smyth)

parameter modification or enforce user-specified equalities. Reduced parametrization, on the other hand, seeks to decrease the number of updating parameters through an intelligent, often automated process. Subset selection [5, 6] produces a reduced set of updating parameters which are (locally) most effective in reducing the modeling errors. Parameter clustering [1, 3, 7–9] has been established as a viable method for grouping model parameters into clusters which are each updated with a single parameter. This relies on machine learning [10] to group model parameters which have similar effects on model-outputs, as measured by sensitivity. In these contexts, it is important to understand the properties of the sensitivity vectors for various model parameters. Parameter clustering has typically been based on natural frequency sensitivities. When this approach is used on symmetric structures, it has produced symmetric clusters [3, 8, 9]. Recently, the authors incorporated both natural frequency and mode shape sensitivities which notably lead to asymmetric clusters [3]. This also has ramifications for subset selection, since parameters are chosen based on their sensitivity vectors and an orthogonalization process will prevent two parameters from being chosen which have the same sensitivities [5].

Beyond sensitivity-based parametrization methods, other applications also benefit from an in-depth understanding of natural frequency and mode shape sensitivities for symmetric structures. Natural frequencies and mode shapes are widely used damage-sensitive features, not only for damage detection, but also for damage localization. Since natural frequencies are not enough to indicate structural damage locations, they are typically used alongside mode shape data to localize structural damage [11–13]. For the same reason, when model updating is used for a structural damage detection application, it usually includes a combination of natural frequencies and mode shapes in an objective function. Since many civil and mechanical structures have at least one plane of symmetry (for design and construction simplicity), it is fundamentally important to understand the effects of parameter changes in symmetric structures. To this end, developing an understanding of natural frequency and mode shape sensitivities will contribute to robust damage detection algorithms and parametrization methods for these special, yet ubiquitous structures.

In this work, natural frequency and mode shape sensitivities are thoroughly explored in the context of structures having at least one plane of symmetry. In Section 2, prior work is reviewed to establish the symmetry and anti-symmetry of mode shapes in symmetric structures. This is then combined with analytical natural frequency and mode shape sensitivity results to show that natural frequency sensitivities are equal (Section 3) and mode shape sensitivities are unequal (Section 4) between symmetric parameters. These techniques are applied to an example symmetric truss in Section 5 with further analysis of mode shape sensitivities for symmetric parameters. Section 6 presents discussion of findings and conclusions.

2. Eigensolution for symmetric structures

The mathematical study of symmetry in structural dynamics began with Glockner [14] who applied group theory to form reduced representations of full structural systems. A symmetric structure can be transformed through a defined set of reflections and rotations, called the symmetry group, to configurations which are identical to the original structure [15]. When a structure exhibits symmetry, its mass and stiffness matrices can be decomposed into similar block-diagonal forms [16]. In vibration analyses of linear structures, this greatly reduces the computational and memory requirements, as the single, large eigendecomposition is transformed into several smaller, separable eigendecompositions [16]. Group theory is the natural vehicle for establishing these transformations, and has seen extensive study in structural dynamics by Kaveh *et al.* [17–20] and Zingoni [15, 21, 22].

In this work, a single type of symmetry is analyzed, namely a single reflection or bilateral symmetry. This corresponds to the C_{1v} symmetry group which comprises two operations: the identity operation e and a single reflection about a vertical plane σ_v. The identity operation is part of any symmetry group, even for asymmetric structures, so it is often disregarded as a trivial transformation [20]. An example of a structure exhibiting C_{1v} symmetry is given in Fig. 1.

Consider a structure which is divided by a reflection plane into left and right substructures, with link elements cut by the plane. At this point, the structure can be general, with different mass, stiffness, and connectivity properties within the left and right substructures. The only requirement which will be put on the structure is that the left and right substructures contain an equal number of degrees-of-freedom (DoFs), at n. The global stiffness matrix $\boldsymbol{K}$ and mass matrix $\boldsymbol{M}$ for the full structure are thus symmetric positive-definite with dimension $N \times N$ where $N = 2n$. The N-element column vector $\boldsymbol{u}$ represents the displacements of the system. The displacement and force vectors can be partitioned into $\boldsymbol{u}^T = \{\boldsymbol{u}_1^T \ \boldsymbol{u}_2^T\}$ and $\boldsymbol{f}^T = \{\boldsymbol{f}_1^T \ \boldsymbol{f}_2^T\}$, respectively. $\boldsymbol{u}_1$ and $\boldsymbol{f}_1$ correspond to displacements and forces on the left substructure, while $\boldsymbol{u}_2$ and $\boldsymbol{f}_2$ correspond to displacements and forces on the right substructure. $\boldsymbol{u}_1$, $\boldsymbol{f}_1$, $\boldsymbol{u}_2$ and $\boldsymbol{f}_2$ are thus equally-sized column vectors with n components.

One way of defining C_{1v} symmetry in a structure is that the displacements and accelerations are symmetric given a symmetric force vector. Note that "symmetry" in this context refers to being unaffected by reflection, not to the typical transpose-symmetry of matrices. If the displacements are symmetric with reflection, then $\boldsymbol{u}^T = \{\boldsymbol{u}_1^T \ \boldsymbol{u}_2^T\} = \{\boldsymbol{u}_2^T \ \boldsymbol{u}_1^T\}$, or $\boldsymbol{u}_1 = \boldsymbol{u}_2$. A more systematic way of representing this operation is through a linear transformation representing reflection, defined as

$$\boldsymbol{T} = \begin{bmatrix} \boldsymbol{0} & \boldsymbol{I} \\ \boldsymbol{I} & \boldsymbol{0} \end{bmatrix} \tag{1}$$

which is symmetric and involutory (i.e. $\boldsymbol{T}^T = \boldsymbol{T}^{-1} = \boldsymbol{T}$). Therefore, stiffness-symmetry is defined such that $\boldsymbol{u} = \boldsymbol{T}\boldsymbol{u}$ given $\boldsymbol{f} = \boldsymbol{T}\boldsymbol{f}$. Substituting these transformations into the stiffness equation gives

$$\boldsymbol{K}\boldsymbol{u} = \boldsymbol{f} \quad \rightarrow \quad \boldsymbol{K}\boldsymbol{T}\boldsymbol{u} = \boldsymbol{T}\boldsymbol{f} \quad \rightarrow \quad \boldsymbol{T}\boldsymbol{K}\boldsymbol{T} = \boldsymbol{K} \tag{2}$$

In other words, the stiffness matrix of a symmetric structure is unaffected by reflection and is indistinguishable when measuring the stiffness of the left or right substructure DoFs. A similar approach can be applied to the mass matrix, where a mass-symmetry is defined such that the acceleration vector is unaffected by reflection: $\ddot{\boldsymbol{u}} = \boldsymbol{T}\ddot{\boldsymbol{u}}$. This is used to satisfy the relation $\boldsymbol{M}\ddot{\boldsymbol{u}} = \boldsymbol{f}$, where $\boldsymbol{f}$ is again symmetric. This leads to $\boldsymbol{T}\boldsymbol{M}\boldsymbol{T} = \boldsymbol{M}$.

The stiffness matrix for this general structure can be written in block-form as

$$\boldsymbol{K} = \begin{bmatrix} \boldsymbol{K}^{(1)} & \boldsymbol{K}^{(2)} \\ \boldsymbol{K}^{(2)T} & \boldsymbol{K}^{(3)} \end{bmatrix} \tag{3}$$

where $\boldsymbol{K}^{(1)}$ and $\boldsymbol{K}^{(3)}$ represent the connectivity within the left and right side DoFs, respectively (intraconnectivity). $\boldsymbol{K}^{(2)}$ and $\boldsymbol{K}^{(2)T}$ represent the connectivity between the left and right side DoFs, respectively (interconnectivity). As with the displacement vector, assume that the block matrices are equal in size with dimension $n \times n$. If the structure is symmetric such that $\boldsymbol{T}\boldsymbol{K}\boldsymbol{T} = \boldsymbol{K}$, then

$$\boldsymbol{T}\boldsymbol{K}\boldsymbol{T} = \begin{bmatrix} \boldsymbol{K}^{(3)} & \boldsymbol{K}^{(2)T} \\ \boldsymbol{K}^{(2)} & \boldsymbol{K}^{(1)} \end{bmatrix} \qquad \rightarrow \qquad \boldsymbol{K}^{(1)} = \boldsymbol{K}^{(3)}; \qquad \boldsymbol{K}^{(2)} = \boldsymbol{K}^{(2)T} \tag{4}$$

A similar result holds for the mass matrix $\boldsymbol{M}$. Intuitively, this means that the stiffness and mass properties are identical between the left and right substructures which are connected by link elements cut by the plane of symmetry. In other words, for a structure to exhibit symmetrical displacement (and acceleration) given a symmetric input force, it must exhibit stiffness (and mass) symmetry. Therefore, the stiffness and mass matrices can be written as

$$\boldsymbol{K} = \begin{bmatrix} \boldsymbol{K}^{(1)} & \boldsymbol{K}^{(2)} \\ \boldsymbol{K}^{(2)} & \boldsymbol{K}^{(1)} \end{bmatrix} \qquad \boldsymbol{M} = \begin{bmatrix} \boldsymbol{M}^{(1)} & \boldsymbol{M}^{(2)} \\ \boldsymbol{M}^{(2)} & \boldsymbol{M}^{(1)} \end{bmatrix} \tag{5}$$

These matrices have a special construction, with two identical blocks along the diagonal and two separate identical blocks along the off-diagonal. This is defined as a Form II matrix, studied by Kaveh and Sayarinejad [17]. Since $\boldsymbol{K}$ and $\boldsymbol{M}$ are symmetric, then so are the block matrices. $\boldsymbol{K}^{(1)}$ corresponds to the stiffness of the substructures on either side of the symmetry plane, while $\boldsymbol{K}^{(2)}$ corresponds to the stiffness of elements linking together the symmetric substructures. Note that this requires a consistent selection of DoFs. In the case of Fig. 1, this required nodal numbering and DoF selection which was isomorphic with reflection.

$\boldsymbol{K}$ and $\boldsymbol{M}$ are used in a generalized eigenvalue problem for finding natural frequencies $\omega = \sqrt{\lambda}$ and mode shapes $\boldsymbol{\phi}$ which satisfy:

$$[\boldsymbol{K} - \lambda\boldsymbol{M}]\boldsymbol{\phi} = \boldsymbol{0} \tag{6}$$

As noted before, $\boldsymbol{K}$ and $\boldsymbol{M}$ can be block-diagonalized via a transformation. Defining an orthogonal matrix $\boldsymbol{P}$ that rotates the space of eigenvectors, then the eigenvalue problem can be rewritten using transformed stiffness ($\bar{\boldsymbol{K}}$) and mass ($\bar{\boldsymbol{M}}$) matrices. Note that the eigenvalues are invariant to this transformation.

$$\boldsymbol{\phi} = \boldsymbol{P}\bar{\boldsymbol{\phi}} \quad \rightarrow \quad [\underbrace{\boldsymbol{P}^T\boldsymbol{K}\boldsymbol{P}}_{\bar{\boldsymbol{K}}} - \lambda \underbrace{\boldsymbol{P}^T\boldsymbol{M}\boldsymbol{P}}_{\bar{\boldsymbol{M}}}]\bar{\boldsymbol{\phi}} = \mathbf{0} \tag{7}$$

If the matrix $\boldsymbol{P}$ is defined as follows, then this block-diagonalizes $\bar{\boldsymbol{K}}$ and $\bar{\boldsymbol{M}}$

$$\boldsymbol{P} = \frac{1}{\sqrt{2}}\begin{bmatrix} \boldsymbol{I} & -\boldsymbol{I} \\ \boldsymbol{I} & \boldsymbol{I} \end{bmatrix} \quad \rightarrow \quad \bar{\boldsymbol{K}} = \begin{bmatrix} \bar{\boldsymbol{K}}^{(1)} & \mathbf{0} \\ \mathbf{0} & \bar{\boldsymbol{K}}^{(2)} \end{bmatrix} = \begin{bmatrix} \boldsymbol{K}^{(1)} + \boldsymbol{K}^{(2)} & \mathbf{0} \\ \mathbf{0} & \boldsymbol{K}^{(1)} - \boldsymbol{K}^{(2)} \end{bmatrix} \tag{8}$$

where $\bar{\boldsymbol{K}}^{(1)}$ and $\bar{\boldsymbol{K}}^{(2)}$ are called the condensed submatrices of $\boldsymbol{K}$ and similar for $\boldsymbol{M}$. Substituting these results into Eq. (7) yields the separable eigenvalue problem:

$$\begin{bmatrix} \bar{\boldsymbol{K}}^{(1)} - \lambda\bar{\boldsymbol{M}}^{(1)} & \mathbf{0} \\ \mathbf{0} & \bar{\boldsymbol{K}}^{(2)} - \lambda\bar{\boldsymbol{M}}^{(2)} \end{bmatrix} \bar{\boldsymbol{\phi}} = \mathbf{0} \tag{9}$$

The eigenvalues satisfy the following relation:

$$\det(\bar{\boldsymbol{K}} - \lambda\bar{\boldsymbol{M}}) = \det(\bar{\boldsymbol{K}}^{(1)} - \lambda\bar{\boldsymbol{M}}^{(1)})\det(\bar{\boldsymbol{K}}^{(2)} - \lambda\bar{\boldsymbol{M}}^{(2)}) = 0 \tag{10}$$

This gives two separable eigendecompositions, where the first set of eigenvalues is denoted as $\{\lambda^{(1)}\}$ with corresponding eigenvectors $\{\bar{\boldsymbol{\phi}}^{(1)}\}$ which satisfy $[\bar{\boldsymbol{K}}^{(1)} - \lambda^{(1)}\bar{\boldsymbol{M}}^{(1)}]\bar{\boldsymbol{\phi}}^{(1)} = \mathbf{0}$. Similarly, the second set of eigenvalues is denoted as $\{\lambda^{(2)}\}$ with corresponding eigenvectors $\{\bar{\boldsymbol{\phi}}^{(2)}\}$ which satisfy $[\bar{\boldsymbol{K}}^{(2)} - \lambda^{(2)}\bar{\boldsymbol{M}}^{(2)}]\bar{\boldsymbol{\phi}}^{(2)} = \mathbf{0}$. The generalized eigenvalues of $\boldsymbol{K}$, $\boldsymbol{M}$, denoted as $\{\lambda(\boldsymbol{K}, \boldsymbol{M})\}$, are then given by the set union of the eigenvalues of the condensed problems:

$$\{\lambda(\boldsymbol{K}, \boldsymbol{M})\} = \{\lambda(\bar{\boldsymbol{K}}, \bar{\boldsymbol{M}})\} = \{\lambda^{(1)}\} \cup \{\lambda^{(2)}\} \tag{11}$$

The eigenvectors of $\boldsymbol{K}$, $\boldsymbol{M}$, denoted as $\{\boldsymbol{\phi}(\boldsymbol{K}, \boldsymbol{M})\}$ can be evaluated from the eigenvectors of the condensed problems after rotation back through $\boldsymbol{P}$. Inserting the i^{th} eigenvalue of the first condensed problem $\lambda_i^{(1)}$ into Eq. (9) yields

$$\bar{\boldsymbol{\phi}}_i = \begin{Bmatrix} \bar{\boldsymbol{\phi}}_i^{(1)} \\ \mathbf{0} \end{Bmatrix} \quad \rightarrow \quad \boldsymbol{\phi}_i = \boldsymbol{P}\bar{\boldsymbol{\phi}}_i = \begin{Bmatrix} \bar{\boldsymbol{\phi}}_i^{(1)} \\ \bar{\boldsymbol{\phi}}_i^{(1)} \end{Bmatrix} \tag{12}$$

where the scalar was dropped because mode shape scaling is arbitrary. This set of eigenvectors is assembled by duplicating the eigenvectors of the first condensed problem. These eigenvectors are thus symmetric, since $\boldsymbol{\phi}_i = \boldsymbol{T}\boldsymbol{\phi}_i$ for all i from the first condensed problem. Since the eigenvectors are symmetric (i.e. unaffected by reflection) the corresponding modes are said to be symmetric modes.

The eigenvector associated with the j^{th} eigenvalue of the second condensed problem, $\lambda_j^{(2)}$ is similarly evaluated as

$$\bar{\boldsymbol{\phi}}_j = \begin{Bmatrix} \mathbf{0} \\ \bar{\boldsymbol{\phi}}_j^{(2)} \end{Bmatrix} \quad \rightarrow \quad \boldsymbol{\phi}_j = \boldsymbol{P}\bar{\boldsymbol{\phi}}_j = \begin{Bmatrix} \bar{\boldsymbol{\phi}}_j^{(2)} \\ -\bar{\boldsymbol{\phi}}_j^{(2)} \end{Bmatrix} \tag{13}$$

where the scalar was again omitted. The eigenvectors are assembled by duplication from the eigenvectors of the condensed problem, but now the two blocks are opposite. These eigenvectors are thus anti-symmetric since $\boldsymbol{\phi}_j = -\boldsymbol{T}\boldsymbol{\phi}_j$ for all j from the second condensed problem. Similar to the symmetric mode shapes, the modes corresponding to anti-symmetric eigenvectors are said to be anti-symmetric modes.

The total set of generalized eigenvectors, $\{\boldsymbol{\phi}(\boldsymbol{K}, \boldsymbol{M})\}$, is then given by the union of those two sets of eigenvectors

$$\{\boldsymbol{\phi}(\boldsymbol{K}, \boldsymbol{M})\} = \begin{Bmatrix} \bar{\boldsymbol{\phi}}^{(1)} \\ \bar{\boldsymbol{\phi}}^{(1)} \end{Bmatrix} \cup \begin{Bmatrix} \bar{\boldsymbol{\phi}}^{(2)} \\ -\bar{\boldsymbol{\phi}}^{(2)} \end{Bmatrix} \tag{14}$$

which takes significant liberty with notation to indicate that it comprises only symmetric and anti-symmetric forms of the condensed problem eigenvectors.

These results are applicable to structures which may exhibit further symmetry, as long as they are decomposable by (at least) one C_{1v} symmetry group which produces Form II $\boldsymbol{K}$ and $\boldsymbol{M}$ matrices, as defined in Eq. (5). Furthermore, this approach can be extended to structures which have DoFs along the line of symmetry. Using the notation of Kaveh and Nikbakht [20], this corresponds to a Form III matrix which is essentially an augmentation of a Form II matrix. The symmetry and anti-symmetry of mode shapes (excluding the DoFs along the line of symmetry) are preserved for Form III matrices. The reflection matrix $\boldsymbol{T}$ becomes more complex in these situations, and further work is warranted to derive the solutions for these structures.

3. Natural frequency sensitivity

Previous applications of group theory to structural dynamics sought to reduce computational expense or memory requirements for the analysis of symmetric structures. In this work, the special properties of mode shapes in symmetric structures are combined with analytical sensitivity results to explore natural frequency and mode shape sensitivities. To simplify notation in the remaining work, λ refers to $\lambda(\boldsymbol{K}, \boldsymbol{M})$ and $\boldsymbol{\phi} = \boldsymbol{\phi}(\boldsymbol{K}, \boldsymbol{M})$. The resulting natural frequency sensitivities can be calculated analytically using the result of Fox and Kapoor [23], which is also derived in Adhikari [24] for arbitrary mode shape normalization and for systems with damping:

$$\lambda_{i,k} = \boldsymbol{\phi}_i^T \boldsymbol{G}_{i,k} \boldsymbol{\phi}_i \tag{15}$$

Note that $\boldsymbol{G}_{i,k} = \boldsymbol{K}_{,k} - \lambda_i \boldsymbol{M}_{,k}$ where $\square_{,k}$ represents the partial derivative with respect to parameter k, $\partial\square/\partial\theta_k$. The term $\boldsymbol{G}_{i,k}$ is evaluated for two parameters, θ_k and θ_l which are symmetric, such that

$$\boldsymbol{K}_{,k} = \begin{bmatrix} \boldsymbol{K}_{,k}^{(1)} & \boldsymbol{0} \\ \boldsymbol{0} & \boldsymbol{0} \end{bmatrix} \qquad \boldsymbol{K}_{,l} = \boldsymbol{T}\boldsymbol{K}_{,k}\boldsymbol{T} = \begin{bmatrix} \boldsymbol{0} & \boldsymbol{0} \\ \boldsymbol{0} & \boldsymbol{K}_{,k}^{(1)} \end{bmatrix} \tag{16}$$

and similar for $\boldsymbol{M}_{,k}$ and $\boldsymbol{M}_{,l}$. This uses the reflection matrix $\boldsymbol{T}$ defined in Eq. (1). Symmetric parameters may be, for example, the mass densities of two symmetrically-located (mirrored) elements. However, the definition is generic and may include groups of parametrized elements which have a mirror group. The only requirement is that the symmetric parameters satisfy $\boldsymbol{K}_{,l} = \boldsymbol{T}\boldsymbol{K}_{,k}\boldsymbol{T}$. Note that the off-diagonal block matrices of $\boldsymbol{K}_{,k}$ and $\boldsymbol{M}_{,k}$ are necessarily zero since they correspond to the stiffness and mass properties, respectively, of link elements. Since link elements are cut by the reflection plane, they are not part of either substructure and are never going to give symmetric parameters. $\boldsymbol{G}_{i,k}$ and $\boldsymbol{G}_{i,l}$ are then formed

$$\boldsymbol{G}_{i,k} = \begin{bmatrix} \boldsymbol{K}_{,k}^{(1)} - \lambda_i \boldsymbol{M}_{,k}^{(1)} & \boldsymbol{0} \\ \boldsymbol{0} & \boldsymbol{0} \end{bmatrix} \qquad \boldsymbol{G}_{i,l} = \boldsymbol{T}\boldsymbol{G}_{i,k}\boldsymbol{T} = \begin{bmatrix} \boldsymbol{0} & \boldsymbol{0} \\ \boldsymbol{0} & \boldsymbol{K}_{,k}^{(1)} - \lambda_i \boldsymbol{M}_{,k}^{(1)} \end{bmatrix} \tag{17}$$

3.1. Symmetric mode shape

As established in Section 2, the mode shapes of symmetric structures are either symmetric or anti-symmetric. Analysis begins with an arbitrary symmetric mode i, such that

$$\boldsymbol{\phi}_i = \begin{Bmatrix} \boldsymbol{v}_i \\ \boldsymbol{v}_i \end{Bmatrix} = \boldsymbol{T}\boldsymbol{\phi}_i \tag{18}$$

for some non-zero vector $\boldsymbol{v}_i$. $\boldsymbol{\phi}_i$ is unaffected by the reflection matrix $\boldsymbol{T}$ in Eq. (1). Writing the eigenvalue sensitivity with respect to parameter θ_l and using the relation in Eq. (17):

$$\lambda_{i,l} = \boldsymbol{\phi}_i^T \boldsymbol{G}_{i,l} \boldsymbol{\phi}_i = \boldsymbol{\phi}_i^T [\boldsymbol{T}\boldsymbol{G}_{i,k}\boldsymbol{T}] \boldsymbol{\phi}_i = [\boldsymbol{\phi}_i^T \boldsymbol{T}] \boldsymbol{G}_{i,k} [\boldsymbol{T}\boldsymbol{\phi}_i] = \boldsymbol{\phi}_i^T \boldsymbol{G}_{i,k} \boldsymbol{\phi}_i = \lambda_{i,k} \tag{19}$$

then equivalence is satisfied, and eigenvalue sensitivities are equal between symmetric parameters for symmetric modes.

3.2. Anti-symmetric mode shape

This examination is repeated for an arbitrary anti-symmetric mode j,

$$\boldsymbol{\phi}_j = \left\{ \begin{array}{c} \boldsymbol{v}_j \\ -\boldsymbol{v}_j \end{array} \right\} = -\boldsymbol{T}\boldsymbol{\phi}_j \tag{20}$$

which is negated when transformed by the reflection matrix $\boldsymbol{T}$ in Eq. (1). The eigenvalue sensitivity with respect to θ_l can again be equated to the sensitivity with respect to θ_k:

$$\lambda_{j,l} = \boldsymbol{\phi}_j^T \boldsymbol{G}_{j,l} \boldsymbol{\phi}_j = \boldsymbol{\phi}_j^T [\boldsymbol{T}\boldsymbol{G}_{j,k}\boldsymbol{T}] \boldsymbol{\phi}_j = [-\boldsymbol{\phi}_j^T \boldsymbol{T}] \boldsymbol{G}_{j,k} [-\boldsymbol{T}\boldsymbol{\phi}_j] = \boldsymbol{\phi}_j^T \boldsymbol{G}_{j,k} \boldsymbol{\phi}_j = \lambda_{j,k} \tag{21}$$

and thus eigenvalue sensitivities are equal between symmetric parameters also for anti-symmetric modes.

Therefore eigenvalue (and correspondingly, natural frequency) sensitivities are equal between symmetric parameters for all modes, comprising symmetric and anti-symmetric modes, in symmetric structures. This is a significant result and gives an analytical explanation for the symmetry of clusters based on natural frequency sensitivity, as noted in [3, 8, 9]. Since natural frequency sensitivity vectors will always be equal between symmetric parameters, they will be clustered together using any distance metric or clustering technique. Furthermore, this means that subset selection based on natural frequency sensitivity will necessarily select against a symmetric parameter after its complement has been chosen. This occurs because the selection process orthogonalizes after each selection, and the identical sensitivity of the parameter pair will be removed.

Finally, this has large ramifications for the sensitivity matrix in sensitivity-based model updating. If an updating problem is set to update only natural frequencies, then two columns corresponding to symmetric parameters will be linearly dependent and the rank of the sensitivity matrix will be less than the number of columns. Therefore, special care must be taken when updating the natural frequencies of symmetric structures to correctly determine the rank of the sensitivity matrix prior to updating and take the correct ameliorating steps of regularization or reparametrization.

4. Mode shape sensitivity

This approach is now extended to mode shape sensitivities. The sensitivity, or derivative, of mode shape $\boldsymbol{\phi}_i$ with respect to parameter θ_k is given by [23]:

$$\boldsymbol{\phi}_{i,k} = -\underbrace{[\boldsymbol{F}_i\boldsymbol{F}_i + 2\boldsymbol{M}\boldsymbol{\phi}_i\boldsymbol{\phi}_i^T\boldsymbol{M}]}_{\boldsymbol{L}_i}{}^{-1} \underbrace{[\boldsymbol{F}_i\boldsymbol{F}_{i,k} + \boldsymbol{M}\boldsymbol{\phi}_i\boldsymbol{\phi}_i^T\boldsymbol{M}_{,k}]}_{\boldsymbol{R}_{i,k}} \boldsymbol{\phi}_i \tag{22}$$

This can be split into the inverse of a symmetric matrix $\boldsymbol{L}_i$ which does not depend on the parameter θ_k, a matrix $\boldsymbol{R}_{i,k}$, and the mode shape $\boldsymbol{\phi}_i$. $\boldsymbol{L}_i$ is Form II, meaning that $\boldsymbol{T}\boldsymbol{L}_i\boldsymbol{T} = \boldsymbol{L}_i$. Thus $\boldsymbol{L}_i^{-1}$ is also Form II ($\boldsymbol{L}_i^{-1} = [\boldsymbol{T}\boldsymbol{L}_i\boldsymbol{T}]^{-1} = \boldsymbol{T}\boldsymbol{L}_i^{-1}\boldsymbol{T}$), giving properties that will be exploited later. $\boldsymbol{F}_i$ represents the eigenvalue problem with eigenvalue λ_i, which has the same form as the $\boldsymbol{K}$ and $\boldsymbol{M}$ matrices:

$$\boldsymbol{F}_i = \boldsymbol{K} - \lambda_i\boldsymbol{M} = \begin{bmatrix} \boldsymbol{F}_i^{(1)} & \boldsymbol{F}_i^{(2)} \\ \boldsymbol{F}_i^{(2)} & \boldsymbol{F}_i^{(1)} \end{bmatrix} \tag{23}$$

The derivative of $\boldsymbol{F}_i$ with respect to parameter θ_k is given as $\boldsymbol{F}_{i,k} = \boldsymbol{K}_{,k} - \lambda_i\boldsymbol{M}_{,k} - \lambda_{i,k}\boldsymbol{M}$, which is closely related to $\boldsymbol{G}_{i,k}$ from Eq. (17):

$$\boldsymbol{F}_{i,k} = \begin{bmatrix} \boldsymbol{F}_{i,k}^{(1)} & \boldsymbol{F}_{i,k}^{(2)} \\ \boldsymbol{F}_{i,k}^{(2)} & \boldsymbol{F}_{i,k}^{(3)} \end{bmatrix} = \boldsymbol{G}_{i,k} - \lambda_{i,k}\boldsymbol{M} \tag{24}$$

The derivative with respect to a symmetric parameter $\boldsymbol{\theta}_l$ is

$$\boldsymbol{F}_{i,l} = \begin{bmatrix} \boldsymbol{F}_{i,l}^{(1)} & \boldsymbol{F}_{i,l}^{(2)} \\ \boldsymbol{F}_{i,l}^{(2)} & \boldsymbol{F}_{i,l}^{(3)} \end{bmatrix} = \boldsymbol{G}_{i,l} - \lambda_{i,k}\boldsymbol{M} \tag{25}$$

where the result $\lambda_{i,l} = \lambda_{i,k}$ was used from Section 3. This means that $\boldsymbol{F}_{i,l}$ is the reflection of $\boldsymbol{F}_{i,k}$, using the reflection matrix in Eq. (1):

$$\boldsymbol{F}_{i,l} = \boldsymbol{T}\boldsymbol{F}_{i,k}\boldsymbol{T} \tag{26}$$

Using these definitions, the goal is to describe the similarity between mode shape sensitivities for two symmetric parameters. Generally, subset selection methods and parameter clustering methods phrase similarity in terms of the cosine distance between vectors [3, 5, 7–9]. Between two mode shape sensitivity vectors, this can be written:

$$d_{\cos}(\boldsymbol{\phi}_{i,k}, \boldsymbol{\phi}_{i,l}) = 1 - \frac{\boldsymbol{\phi}_{i,k}^T \boldsymbol{\phi}_{i,l}}{\sqrt{\boldsymbol{\phi}_{i,k}^T \boldsymbol{\phi}_{i,k} \cdot \boldsymbol{\phi}_{i,l}^T \boldsymbol{\phi}_{i,l}}} \tag{27}$$

This is equal to $1 - \cos(\psi)$ where ψ is the angle between the two vectors. $d_{\cos}$ ranges between 0 (vectors are parallel) and 2 (vectors are anti-parallel). When $\boldsymbol{\phi}_{i,k}$ and $\boldsymbol{\phi}_{i,l}$ have the same magnitude (i.e. $\boldsymbol{\phi}_{i,k}^T \boldsymbol{\phi}_{i,k} = \boldsymbol{\phi}_{i,l}^T \boldsymbol{\phi}_{i,l}$), then this can be written as

$$d_{\cos}(\boldsymbol{\phi}_{i,k}, \boldsymbol{\phi}_{i,l}) = \{\boldsymbol{\phi}_{i,k} - \boldsymbol{\phi}_{i,l}\}^T \{\boldsymbol{\phi}_{i,k} - \boldsymbol{\phi}_{i,l}\} / (2\boldsymbol{\phi}_{i,k}^T \boldsymbol{\phi}_{i,k}) \tag{28}$$

In order for two symmetric parameters, θ_k and θ_l, to have $d_{\cos} = 0$ when using Eq. (28) then the following condition must hold:

$$\boldsymbol{\phi}_{i,k} - \boldsymbol{\phi}_{i,l} = -\boldsymbol{L}_i^{-1}[\boldsymbol{R}_{i,k}\boldsymbol{\phi}_i - \boldsymbol{R}_{i,l}\boldsymbol{\phi}_i] = \boldsymbol{0} \quad \rightarrow \quad \boldsymbol{R}_{i,k}\boldsymbol{\phi}_i - \boldsymbol{R}_{i,l}\boldsymbol{\phi}_i = \boldsymbol{0} \tag{29}$$

where $\boldsymbol{L}_i^{-1}$ can be reduced because it is invertible.

4.1. Symmetric mode shape

Eq. (29) is analyzed in the context of a symmetric mode shape, $\boldsymbol{\phi}_i$, with form given by Eq. (18). However, we will first show that the symmetric parameter sensitivities are equal in magnitude to allow use of Eq. (28). To do this, Eq. (22) is examined for mode i and parameter l:

$$\begin{aligned} \boldsymbol{R}_{i,l}\boldsymbol{\phi}_i &= [\boldsymbol{F}_i\boldsymbol{F}_{i,l} + \boldsymbol{M}\boldsymbol{\phi}_i\boldsymbol{\phi}_i^T\boldsymbol{M}_{,l}]\boldsymbol{\phi}_i = [\boldsymbol{F}_i[\boldsymbol{T}\boldsymbol{F}_{i,k}\boldsymbol{T}] + \boldsymbol{M}\boldsymbol{\phi}_i\boldsymbol{\phi}_i^T[\boldsymbol{T}\boldsymbol{M}_{,k}\boldsymbol{T}]]\boldsymbol{\phi}_i \\ &= [\boldsymbol{F}_i\boldsymbol{T}\boldsymbol{F}_{i,k} + \boldsymbol{M}\boldsymbol{\phi}_i\boldsymbol{\phi}_i^T\boldsymbol{T}\boldsymbol{M}_{,k}]\boldsymbol{T}\boldsymbol{\phi}_i = [\boldsymbol{F}_i\boldsymbol{T}\boldsymbol{F}_{i,k} + \boldsymbol{M}\boldsymbol{\phi}_i\boldsymbol{\phi}_i^T\boldsymbol{M}_{,k}]\boldsymbol{\phi}_i \end{aligned} \tag{30}$$

This uses the reflection matrix $\boldsymbol{T}$ in Eq. (1) to describe the transformations of $\boldsymbol{F}_{i,l}$ in Eq. (26) and $\boldsymbol{M}_{,l}$, similar to Eq. (16). This is further simplified using the fact that $\boldsymbol{T}\boldsymbol{\phi}_i = \boldsymbol{\phi}_i$ for a symmetric mode shape. Given that $\boldsymbol{L}_i^{-1}$ is a Form II matrix, then $\boldsymbol{T}\boldsymbol{L}_i^{-1} = \boldsymbol{L}_i^{-1}\boldsymbol{T}$. Thus, we can show that $\boldsymbol{T}\boldsymbol{\phi}_{i,k} = \boldsymbol{\phi}_{i,l}$ using a part of Eq. (22) and Eq. (30):

$$\boldsymbol{T}\boldsymbol{\phi}_{i,k} = -\boldsymbol{L}_i^{-1}\boldsymbol{T}\boldsymbol{R}_{i,k}\boldsymbol{\phi}_i = -\boldsymbol{L}_i^{-1}[\boldsymbol{F}_i\boldsymbol{T}\boldsymbol{F}_{i,k} + \boldsymbol{M}\boldsymbol{\phi}_i\boldsymbol{\phi}_i^T\boldsymbol{M}_{,k}]\boldsymbol{\phi}_i = \boldsymbol{\phi}_{i,l} \tag{31}$$

This utilizes the facts that $\boldsymbol{F}_i$ and $\boldsymbol{M}$ are Form II to give $\boldsymbol{T}\boldsymbol{F}_i = \boldsymbol{F}_i\boldsymbol{T}$ and $\boldsymbol{T}\boldsymbol{M} = \boldsymbol{M}\boldsymbol{T}$. Therefore the two sensitivity vectors have equal magnitude, $\boldsymbol{\phi}_{i,l}^T\boldsymbol{\phi}_{i,l} = \boldsymbol{\phi}_{i,k}^T\boldsymbol{T}\boldsymbol{T}\boldsymbol{\phi}_{i,k} = \boldsymbol{\phi}_{i,k}^T\boldsymbol{\phi}_{i,k}$, so Eq. (28) can be used.

Comparing Eq. (30) to $\boldsymbol{R}_{i,k}\boldsymbol{\phi}_i$ in Eq. (22) gives the following relation to satisfy Eq. (29):

$$[\boldsymbol{F}_i - \boldsymbol{F}_i\boldsymbol{T}]\boldsymbol{F}_{i,k}\boldsymbol{\phi}_i = \boldsymbol{0} \tag{32}$$

Note that $\boldsymbol{F}_i$ can not be reduced from this equation since it is not invertible. For a particular mode shape $\boldsymbol{\phi}_i$ and parameter θ_k, this equation may be satisfied by several $\boldsymbol{F}_i$ because $\boldsymbol{F}_{i,k}$ isn't necessarily full-rank. However, this equation must hold for any arbitrary parameter θ_k. Therefore, $\boldsymbol{F}_{i,k}$ can be treated as an arbitrary matrix because the $\boldsymbol{K}_{,k}$ and $\boldsymbol{M}_{,k}$ are arbitrary based on parametrization. Since $\boldsymbol{\phi}_i$ is necessarily non-zero by definition of an eigenvector, the only general solution is $\boldsymbol{F}_i = \boldsymbol{F}_i\boldsymbol{T}$. This requirement can be written as $\boldsymbol{F}_i^{(1)} = \boldsymbol{F}_i^{(2)}$ from Eq. (23):

$$\boldsymbol{K}^{(1)} - \lambda_i\boldsymbol{M}^{(1)} = \boldsymbol{K}^{(2)} - \lambda_i\boldsymbol{M}^{(2)} \tag{33}$$

This may have infinitely many solutions for a particular eigenvalue λ_i, but it is desired to find a condition such that mode shape sensitivities are equal for symmetric parameters *for all symmetric modes*. Therefore, λ_i is treated as arbitrary, giving the requirements that

$$\boldsymbol{K}^{(1)} = \boldsymbol{K}^{(2)} \qquad \boldsymbol{M}^{(1)} = \boldsymbol{M}^{(2)} \tag{34}$$

While generally difficult to attain, this condition doesn't violate any properties of the stiffness and mass matrices (i.e. symmetry, non-zero).

4.2. Anti-symmetric mode shape

Eq. (29) is now analyzed in the context of an anti-symmetric mode shape, $\boldsymbol{\phi}_j$, with form given by Eq. (20). Again, it is first shown that the symmetric parameters have equal magnitude sensitivity vectors by examining part of Eq. (22) This is simplified using $\boldsymbol{T}\boldsymbol{\phi}_j = -\boldsymbol{\phi}_j$ for an anti-symmetric mode shape:

$$\begin{aligned} \boldsymbol{R}_{j,l}\boldsymbol{\phi}_j &= [\boldsymbol{F}_j\boldsymbol{F}_{j,l} + \boldsymbol{M}\boldsymbol{\phi}_j\boldsymbol{\phi}_j^T\boldsymbol{M}_{,l}]\boldsymbol{\phi}_j = [\boldsymbol{F}_j[\boldsymbol{T}\boldsymbol{F}_{j,k}\boldsymbol{T}] + \boldsymbol{M}\boldsymbol{\phi}_j\boldsymbol{\phi}_j^T[\boldsymbol{T}\boldsymbol{M}_{,k}\boldsymbol{T}]]\boldsymbol{\phi}_j \\ &= [\boldsymbol{F}_j\boldsymbol{T}\boldsymbol{F}_{j,k} + \boldsymbol{M}\boldsymbol{\phi}_j\boldsymbol{\phi}_j^T\boldsymbol{T}\boldsymbol{M}_{,k}]\boldsymbol{T}\boldsymbol{\phi}_j = -[\boldsymbol{F}_j\boldsymbol{T}\boldsymbol{F}_{j,k} - \boldsymbol{M}\boldsymbol{\phi}_j\boldsymbol{\phi}_j^T\boldsymbol{M}_{,k}]\boldsymbol{\phi}_j \end{aligned} \tag{35}$$

This can be used to show that $\boldsymbol{\phi}_{j,l} = -\boldsymbol{T}\boldsymbol{\phi}_{j,k}$ in a similar process to Eq. (31). Thus, two sensitivity vectors have equal magnitude, $\boldsymbol{\phi}_{j,l}^T\boldsymbol{\phi}_{j,l} = \boldsymbol{\phi}_{j,k}^T\boldsymbol{\phi}_{j,k}$, so Eq. (28) can be used. Comparing Eq. (35) to Eq. (29) for mode j gives the following condition such that Eq. (29) is satisfied:

$$[\boldsymbol{F}_j + \boldsymbol{F}_j\boldsymbol{T}]\boldsymbol{F}_{j,k}\boldsymbol{\phi}_j = \boldsymbol{0} \tag{36}$$

As discussed previously, this equation has to hold for an arbitrary parameter θ_k and non-zero $\boldsymbol{\phi}_j$, making $\boldsymbol{F}_{j,k}\boldsymbol{\phi}_j$ an arbitrary vector. The only solution, then, is $\boldsymbol{F}_j = -\boldsymbol{F}_j\boldsymbol{T}$, or equivalently, $\boldsymbol{F}_j^{(1)} = -\boldsymbol{F}_j^{(2)}$. This can be written as

$$\boldsymbol{K}^{(1)} - \lambda_j\boldsymbol{M}^{(1)} = -[\boldsymbol{K}^{(2)} - \lambda_j\boldsymbol{M}^{(2)}] \tag{37}$$

Since this must hold for various values of λ_j, corresponding to different anti-symmetric modes, the only solution which satisfies $\boldsymbol{\phi}_{j,k} = \boldsymbol{\phi}_{j,l}$ for arbitrary (symmetric) parameters θ_k and θ_l and arbitrary anti-symmetric mode j is

$$\boldsymbol{K}^{(1)} = -\boldsymbol{K}^{(2)} \qquad \boldsymbol{M}^{(1)} = -\boldsymbol{M}^{(2)} \tag{38}$$

Comparing the equivalence criterion for symmetric mode shapes in Eq. (34) and anti-symmetric Eq. (38) yields the only solution to both sets: $\boldsymbol{K}^{(1)} = \boldsymbol{K}^{(2)} = \boldsymbol{0}$ and $\boldsymbol{M}^{(1)} = \boldsymbol{M}^{(2)} = \boldsymbol{0}$, which is a null result. Therefore, we have analytically shown that there is no symmetric structure for which all mode shape sensitivities will be equal between symmetric parameters, in direct contrast to natural frequency sensitivities, which will be equal. In other words, the presence of structural symmetry is never going to let symmetric parameters have the same mode shape sensitivities. Intuitively, one would expect that the more closely mode shape sensitivity equivalence is satisfied for symmetric modes, the greater discrepancy would exist for anti-symmetric modes, and vice versa. This comes from observation of Eqs. (32) and (36), but $\boldsymbol{L}_i^{-1}$, $\boldsymbol{F}_{i,k}$, and $\boldsymbol{\phi}_i$ will vary for each mode, so it is not guaranteed that this condition will exist.

However, the observation that $d_{\cos}(\boldsymbol{\phi}_{i,k}, \boldsymbol{\phi}_{i,l}) > 0$ is limited in utility. While the cosine distance between mode shape sensitivities for symmetric parameters is necessarily greater than zero, the cosine distance may still be close enough to zero such that symmetric parameters are still clustered together (in cluster analysis) or nearly orthogonalized (in subset selection) or essentially linearly dependent (in the sensitivity matrix). Since the equations do not readily admit a bound on $d_{\cos}$, this will be explored in a small numerical study.

5. Example structure with C_{1v} symmetry

The structure of study, in Fig. 1, was modified from Kaveh and Nikbakht [20]. This is a symmetric 10 element truss formed from two equilateral triangles (elements $\{1, 2, 3\}$ and elements $\{8, 9, 10\}$) with link elements $\{4, 5, 6, 7\}$. The element properties are uniform, with dimensionless Young's modulus of 1, area 1, and mass density 1. The structure is pinned at the symmetric nodes 1 and 4, giving 8 free DoFs. Note that DoFs 5 and 7 are reversed relative to the direction of 1 and 3 such that DoFs 5-8 are isomorphic to DoFs 1-4 after reflection, giving the structure C_{1v} symmetry. The displacements of the structure are thus partitioned as

$$\boldsymbol{u}^T = \left\{\boldsymbol{u}_1^T \mid \boldsymbol{u}_2^T\right\} = \{u_1\ u_2\ u_3\ u_4 \mid u_5\ u_6\ u_7\ u_8\} \tag{39}$$

corresponding to left and right substructures. The stiffness $\boldsymbol{K}$ and mass $\boldsymbol{M}$ matrices are Form II, as described

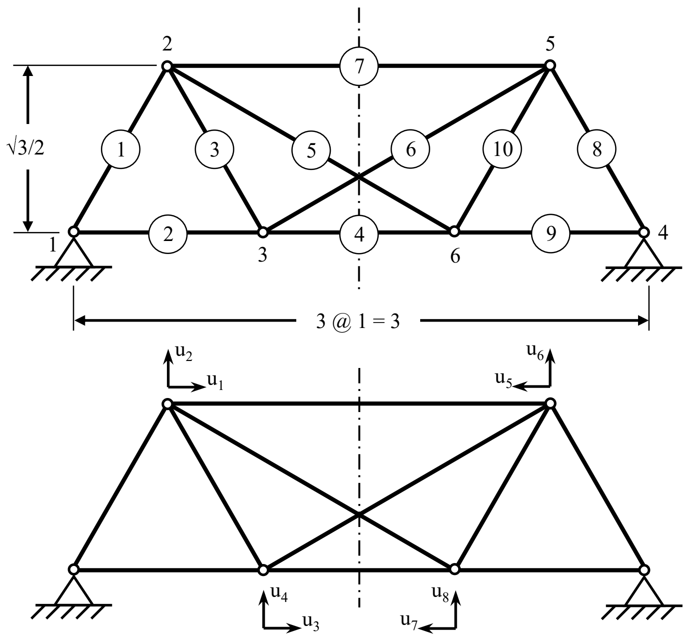

Figure 1: Symmetric 8-DoF truss structure adapted from Kaveh and Nikbakht [20]

in Eq. (5) with block matrices given by

$$\boldsymbol{K} = \left[\begin{array}{c|c} \boldsymbol{K}^{(1)} & \boldsymbol{K}^{(2)} \\ \hline \boldsymbol{K}^{(2)} & \boldsymbol{K}^{(1)} \end{array}\right] = \left[\begin{array}{rrrr|rrrr} 1.43 & -0.25 & -0.25 & 0.43 & 0.50 & 0 & 0.43 & 0.25 \\ -0.25 & 1.64 & 0.43 & -0.75 & 0 & 0 & -0.25 & -0.14 \\ -0.25 & 0.43 & 2.68 & -0.18 & 0.43 & -0.25 & 1 & 0 \\ 0.43 & -0.75 & -0.18 & 0.89 & 0.25 & -0.14 & 0 & 0 \\ \hline 0.50 & 0 & 0.43 & 0.25 & 1.43 & -0.25 & -0.25 & 0.43 \\ 0 & 0 & -0.25 & -0.14 & -0.25 & 1.64 & 0.43 & -0.75 \\ 0.43 & -0.25 & 1 & 0 & -0.25 & 0.43 & 2.68 & -0.18 \\ 0.25 & -0.14 & 0 & 0 & 0.43 & -0.75 & -0.18 & 0.89 \end{array}\right] \tag{40}$$

$$\boldsymbol{M} = \left[\begin{array}{c|c} \boldsymbol{M}^{(1)} & \boldsymbol{M}^{(2)} \\ \hline \boldsymbol{M}^{(2)} & \boldsymbol{M}^{(1)} \end{array}\right] = \left[\begin{array}{rrrr|rrrr} 1.91 & 0 & 0.17 & 0 & -0.33 & 0 & -0.29 & 0 \\ 0 & 1.91 & 0 & 0.17 & 0 & 0.33 & 0 & 0.29 \\ 0.17 & 0 & 1.58 & 0 & -0.29 & 0 & -0.17 & 0 \\ 0 & 0.17 & 0 & 1.58 & 0 & 0.29 & 0 & 0.17 \\ \hline -0.33 & 0 & -0.29 & 0 & 1.91 & 0 & 0.17 & 0 \\ 0 & 0.33 & 0 & 0.29 & 0 & 1.91 & 0 & 0.17 \\ -0.29 & 0 & -0.17 & 0 & 0.17 & 0 & 1.58 & 0 \\ 0 & 0.29 & 0 & 0.17 & 0 & 0.17 & 0 & 1.58 \end{array}\right] \tag{41}$$

Transforming these matrices by $\boldsymbol{P}$ in Eq. (8) to be block-diagonal yields the condensed matrices $\bar{\boldsymbol{K}}^{(1)}$, $\bar{\boldsymbol{K}}^{(2)}$, $\bar{\boldsymbol{M}}^{(1)}$ and $\bar{\boldsymbol{M}}^{(2)}$. This leads to the separable eigenvalue problem in Eq. (9), which give the eigenvalues of $\boldsymbol{K}$

and $\boldsymbol{M}$ as the union of the eigenvalues for the condensed problems:

$$\{\lambda^{(1)}\} = \{0.08,\ 0.88,\ 1.76,\ 2.70\} \qquad \{\lambda^{(2)}\} = \{0.19,\ 0.42,\ 0.83,\ 1.81\} \tag{42}$$

Therefore, the eigenvalues are $\{\lambda\} = \{0.08,\ 0.19,\ 0.42,\ 0.83,\ 0.88,\ 1.76,\ 1.81,\ 2.70\}$ with modes 1, 5, 6, and 8 coming from the first condensed problem (symmetric) and modes 2, 3, 4, and 7 from the second condensed problem (anti-symmetric). The associated eigenvectors for the separable problems are

$$\bar{\boldsymbol{\phi}}^{(1)} = \begin{bmatrix} -0.30 & 1 & 1 & 0.20 \\ 0.58 & 0.77 & -0.82 & 0.05 \\ 0.04 & -0.21 & -0.06 & 1 \\ 1 & -0.42 & 0.96 & -0.04 \end{bmatrix} \qquad \bar{\boldsymbol{\phi}}^{(2)} = \begin{bmatrix} 1 & 0.31 & 0.59 & -0.57 \\ -0.33 & 0.63 & 1 & 0.80 \\ 0.68 & 0.02 & -0.90 & 1 \\ -0.40 & 1 & -0.84 & -0.36 \end{bmatrix} \tag{43}$$

These can be transformed into the eigenvectors of the full problem using Eq. (7), which are separated into

$$\boldsymbol{\phi} = \begin{bmatrix} \bar{\boldsymbol{\phi}}^{(1)} & \bar{\boldsymbol{\phi}}^{(2)} \\ \bar{\boldsymbol{\phi}}^{(1)} & -\bar{\boldsymbol{\phi}}^{(2)} \end{bmatrix} \tag{44}$$

Note that this doesn't reflect the typical mode ordering (based on ascending eigenvalue), but is used to show that the mode shapes are symmetric and anti-symmetric. The mode shapes are depicted in Fig. 2.

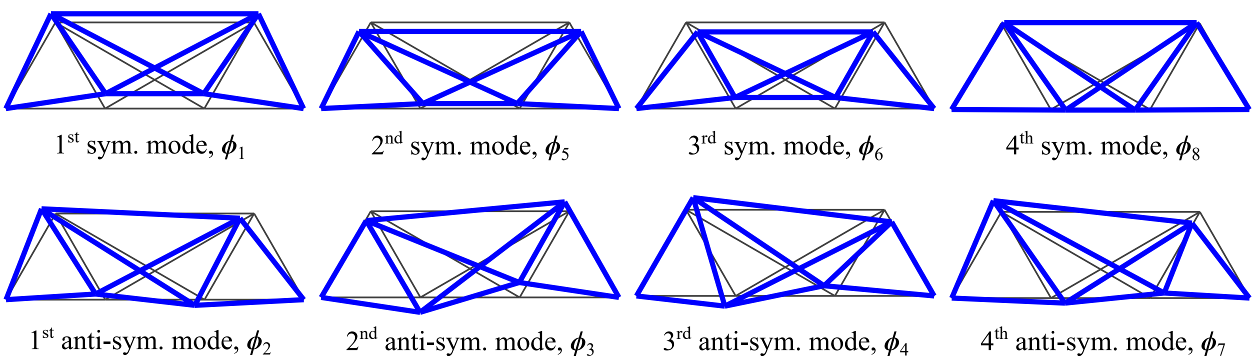

Figure 2: Truss mode shapes

The model was parametrized to modify the stiffness (or equivalently, Young's modulus) of each element l out of a total $p = 10$

$$\boldsymbol{K}(\boldsymbol{\theta}) = \sum_{l=1}^{p} \boldsymbol{K}_l(1 - \theta_l) \tag{45}$$

where $\boldsymbol{\theta}$ is the vector of parameters and $\boldsymbol{K}_l$ is the element stiffness matrix of element l. Therefore, the derivatives are simple, with $\boldsymbol{K}_{,l} = -\boldsymbol{K}_l$ and $\boldsymbol{M}_{,l} = \boldsymbol{0}$. The parameter sets $\{1, 8\}$, $\{2, 9\}$, and $\{3, 10\}$ were symmetric.

The natural frequency sensitivities and mode shape sensitivities were computed numerically for the purposes of verification. A selection of these mode shape sensitivities for symmetric parameters are shown in Fig. 3. The parameter (element) is indicated with a bold line while the sensitivity is indicated by a red arrow for each DoF. This represents how the mode shape changes as a result of perturbing the indicated parameter. The numerically-computed sensitivities obeyed the reflection properties noted in Section 4, with $\boldsymbol{\phi}_{1,1} = \boldsymbol{T}\boldsymbol{\phi}_{1,8}$ and $\boldsymbol{\phi}_{2,3} = -\boldsymbol{T}\boldsymbol{\phi}_{2,10}$. In words, mode shape sensitivities for symmetric parameters are reflections for a symmetric mode, while they are negative reflections for anti-symmetric modes. Visually, $\boldsymbol{\phi}_{1,1}$ and $\boldsymbol{\phi}_{1,8}$ appear to be near-opposite, with most of the sensitivities having opposite direction between the two parameters. Conversely, $\boldsymbol{\phi}_{2,3}$ and $\boldsymbol{\phi}_{2,10}$ appear quite similar, especially for the large magnitude terms on nodes 3 and 6.

To quantify the similarity between sensitivity vectors, the cosine distance between mode shape sensitivities was computed between all parameter pairs using Eq. (27). This comprised $p(p-1)/2 = 45$ unique pairs

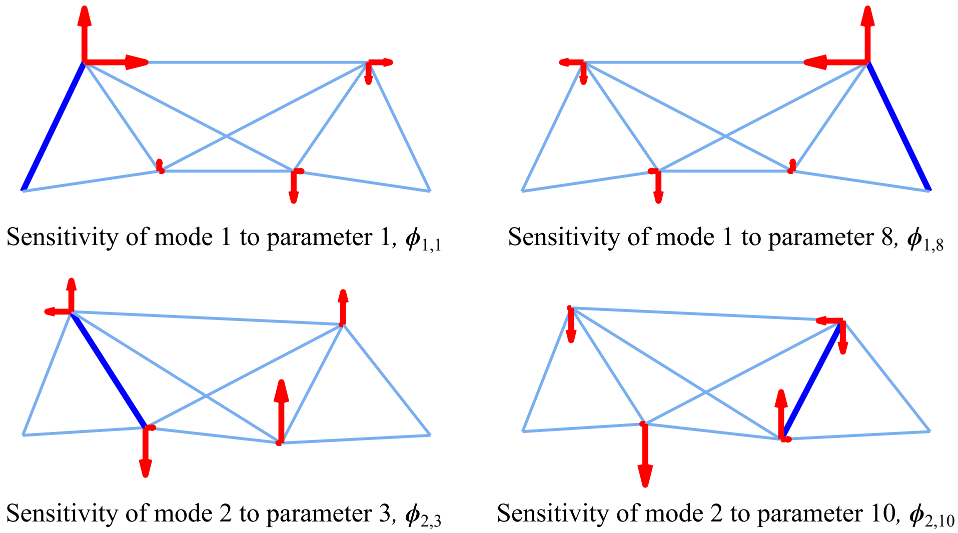

Figure 3: Selected mode shape sensitivities for symmetric parameters

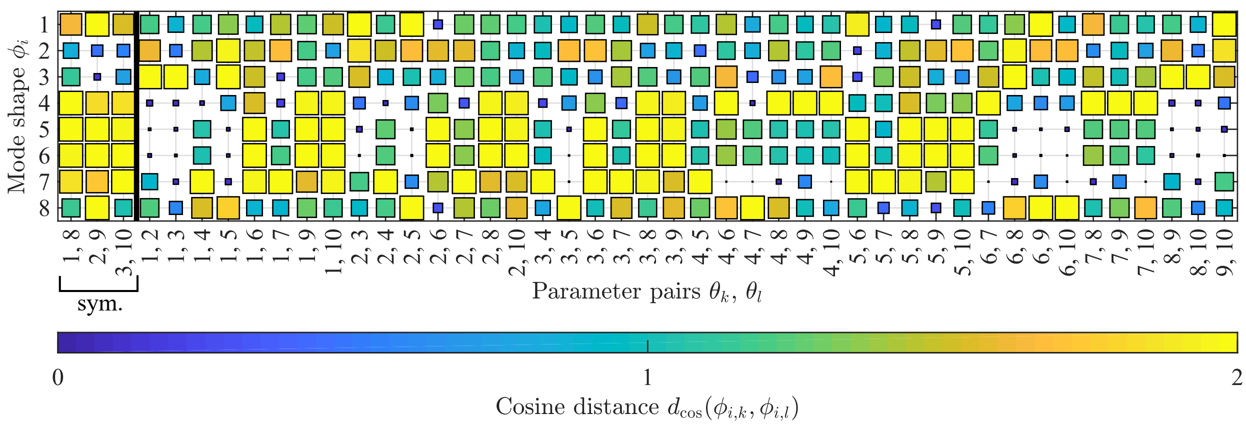

Figure 4: Cosine distances between parameter pairs, separated into symmetric pairs and all other pairs

of parameters, of which 3 represented the symmetric parameter pairs. This was performed for all 8 modes, with results shown in Fig. 4. This allowed for a limited comparison of cosine distance between mode shape sensitivities for symmetric parameter pairs and for all other pairs.

The cosine distance between mode shape sensitivities for the three symmetric parameter pairs was largely similar to the behavior for any other parameter pair. For all symmetric parameter pairs, $d_{\cos}$ was near its maximum for modes 1 and 4-8, showing little preference between symmetric and anti-symmetric mode shapes. A maximal value of $d_{\cos} = 2$ indicated that the mode shapes sensitivities were opposites, as discussed in $\boldsymbol{\phi}_{1,1}$ and $\boldsymbol{\phi}_{1,8}$ of Fig. 3. Conversely, lower values of $d_{\cos}$ can be noted for the symmetric parameter pairs on modes 2 and 3. In particular, $d_{\cos}(\boldsymbol{\phi}_{2,3}, \boldsymbol{\phi}_{2,10})$ was quite small (≈ 0.14), as suggested in the discussion of Fig. 3.

The other 42 parameter pairs showed largely uniform behavior for modes 1-3 and 8, with few values below 1. Conversely, modes 4-7 showed a large proportion of extreme values, having many pairs with $d_{\cos}$ near zero and also near 2. This doesn't seem to indicate a difference between symmetric and anti-symmetric mode shape sensitivity behavior, as these distinct behaviors encompassed both symmetric and anti-symmetric modes.

The mean of $d_{\cos}$ (across all modes) for the symmetric parameter pairs was approximately 1.5, while it was near 1.1 for the other parameter pairs. While this indicates that symmetric parameter pairs are more likely to exhibit significantly different mode shape sensitivities, this is not a guarantee. Symmetric parameter pairs still exhibited significant variability, with $d_{\cos}$ values noted near zero as well as near 2. This is an important result, as it indicates that there are no special properties (e.g. equality, negation) of mode shape sensitivities between symmetric parameters. For the purposes of clustering and subset selection, symmetric parameters aren't expected to exhibit different behavior than any arbitrary pair of parameters. Therefore, they are expected to contribute to asymmetry in clustering and prevent orthogonalization of symmetric parameters in subset selection. For sensitivity-based updating, they are expected to behave like any other parameter pair, with no reason to suspect that they won't contribute to the column-space (rank) of the sensitivity matrix.

6. Conclusions

The properties of natural frequency and mode shape sensitivities were explored in the context of structures possessing at least one plane of reflectional symmetry. For these structures, it was shown that the stiffness and mass matrices can be partitioned into a special form, which reduces the eigenvalue problems into two smaller problems. The reduced problems provide exclusively symmetric or anti-symmetric mode shapes for the symmetric structure. The special symmetry properties of the mode shapes were then used to explore the derivatives (or sensitivities) of natural frequencies and mode shapes to changes in symmetric parameters. It was analytically proved that natural frequency sensitivities are necessarily equal between symmetric parameters, while mode shape sensitivity vectors are always unequal. These topics were applied to a small example truss with symmetry to quantify the difference between mode shape sensitivity vectors, as measured by cosine distance. It was noted that symmetric parameters generally had greater cosine distance between their mode shape sensitivity vectors, as compared to other (asymmetric) parameter pairs, but still exhibited significant variability.

For sensitivity-based clustering, this proves that using natural frequency sensitivities will lead to symmetric clusters, while incorporating mode shape sensitivities will tend to create asymmetric clusters, as observed previously by the authors [3]. This stems from mode shape sensitivities being necessarily unequal between symmetric parameters, while natural frequency sensitivities are always equal between symmetric parameters. For parameter subset selection (which uses the sensitivity matrix), if natural frequency sensitivities are used exclusively, then only one of a pair of symmetric parameters can possibly be chosen, as its counterpart will be orthogonalized. However, incorporating mode shape sensitivity will differentiate the sensitivities of the symmetric parameters, possibly allowing both parameters to be selected. This has similar ramifications for sensitivity-based updating, where use of natural frequency sensitivities will necessarily lead to linearly dependent columns of the sensitivity vector, since the sensitivity vectors for symmetric parameters will be equal. Using mode shape data, with or without natural frequency data, is expected to ameliorate this problem and improve the rank of the sensitivity matrix.

The derived results were validated on the example problem, but the degree of variability between mode shape sensitivities corresponding to symmetric parameters deserves further investigation on a variety of structures.

Acknowledgments

The authors gratefully acknowledge Columbia University's Graduate School of Arts and Sciences in support of the first author through the Guggenheim and Presidential Fellowships. This work was partially supported by the U.S. National Science Foundation (Grant No. CMMI-1563364).

References

[1] J. E. Mottershead, M. Link, M. I. Friswell, The sensitivity method in finite element model updating: a tutorial, Mech. Syst. Signal Process. 25 (7) (2011) 2275–2296. doi:10.1016/j.ymssp.2010.10.012.

[2] E. Simoen, G. De Roeck, G. Lombaert, Dealing with uncertainty in model updating for damage assessment: a review, Mech. Syst. Signal Process. 56–57 (2015) 123–149. doi:10.1016/j.ymssp.2014.11.001.

[3] D. T. Bartilson, J. Jang, A. W. Smyth, Finite element model updating using objective-consistent sensitivity-based parameter clustering and Bayesian regularization, Mech. Syst. Signal Process. 114 (2019) 328–345. doi:10.1016/j.ymssp.2018.05.024.

[4] H. Ahmadian, J. E. Mottershead, M. I. Friswell, Regularisation methods for finite element model updating, Mech. Syst. Signal Process. 12 (1) (1998) 47–64. doi:10.1006/mssp.1996.0133.

[5] M. I. Friswell, J. E. Mottershead, H. Ahmadian, Combining subset selection and parameter constraints in model updating, J. Vib. Acoust. 120 (4) (1998) 854–859. doi:10.1115/1.2893911.

[6] G. Lallement, J. Piranda, Localization methods for parametric updating of finite element models in elastodynamics, in: International Modal Analysis Conference, 8th, 1990, pp. 579–585.

[7] H. Shahverdi, C. Mares, W. Wang, J. E. Mottershead, Clustering of parameter sensitivities: examples from a helicopter airframe model updating exercise, Shock Vib. 16 (1) (2009) 75–87. doi:10.3233/SAV-2009-0455.

[8] J. Jang, A. W. Smyth, Model updating of a full-scale FE model with nonlinear constraint equations and sensitivity-based cluster analysis for updating parameters, Mech. Syst. Signal Process. 83 (2017) 337–355. doi:10.1016/j.ymssp.2016.06.018.

[9] J. Jang, A. W. Smyth, Bayesian model updating of a full-scale finite element model with sensitivity-based clustering, Struct. Control Health Monit. 24 (11) (2017) e2004. doi:10.1002/stc.2004.

[10] L. Rokach, O. Maimon, Clustering Methods, Springer, Boston, 2005, Ch. 15, pp. 321–352. doi:10.1007/0-387-25465-X_15.

[11] O. S. Salawu, Detection of structural damage through changes in frequency: a review, Eng. Struct. 19 (9) (1997) 718–723. doi:10.1016/S0141-0296(96)00149-6.

[12] N. Bicanic, H.-P. Chen, Damage identification in framed structures using natural frequencies, Int. J. Numer. Meth. Eng. 40 (23) (1997) 4451–4468. doi:10.1002/(SICI)1097-0207(19971215)40:23<4451::AID-NME269>3.0.CO;2-L.

[13] H.-P. Chen, Structural damage identification from measured vibration modal data, Ph.D. thesis, Department of Civil Engineering, University of Glasgow, UK (1998).

[14] P. G. Glockner, Symmetry in structural mechanics, J. Struct. Div. ASCE 99 (1) (1973) 71–89.

[15] A. Zingoni, Group-theoretic exploitations of symmetry in computational solid and structural mechanics, Int. J. Numer. Meth. Eng. 79 (3) (2009) 253–289. doi:10.1002/nme.2576.

[16] T. J. Healey, J. A. Treacy, Exact block diagonalization of large eigenvalue problems for structures with symmetry, Int. J. Numer. Meth. Eng. 31 (2) (1991) 265–285. doi:10.1002/nme.1620310205.

[17] A. Kaveh, M. A. Sayarinejad, Eigensolutions for matrices of special structures, Commun. Numer. Meth. Eng. 19 (2003) 125–136. doi:10.1002/cnm.576.

[18] A. Kaveh, B. Salimbahrami, Eigensolution of symmetric frames using graph factorization, Commun. Numer. Meth. Eng. 20 (12) (2004) 889–910. doi:10.1002/cnm.711.

[19] A. Kaveh, M. A. Sayarinejad, Graph symmetry and dynamic systems, Comput. Struct. 82 (23-26) (2004) 2229–2240. doi:10.1016/j.compstruc.2004.03.066.

[20] A. Kaveh, M. Nikbakht, Decomposition of symmetric mass–spring vibrating systems using groups, graphs and linear algebra, Commun. Numer. Meth. Eng. 23 (7) (2007) 639–664. doi:10.1002/cnm.913.

[21] A. Zingoni, On group-theoretic computation of natural frequencies for spring–mass dynamic systems with rectilinear motion, Commun. Numer. Meth. Eng. 24 (11) (2008) 973–987. doi:10.1002/cnm.1003.

[22] A. Zingoni, Group-theoretic insights on the vibration of symmetric structures in engineering, Phil. Trans. R. Soc. A 372 (2008) (2014) 20120037. doi:10.1098/rsta.2012.0037.

[23] R. L. Fox, M. P. Kapoor, Rates of change of eigenvalues and eigenvectors, AIAA J. 6 (12) (1968) 2426–2429. doi:10.2514/3.5008.

[24] S. Adhikari, Rates of change of eigenvalues and eigenvectors in damped dynamic system, AIAA J. 37 (11) (1999) 1452–1458. doi:10.2514/2.622.